Contribution from the Department of Inorganic Chemistry,
Indian Association for the Cultivation of Science, Calcutta 700032, India

Chemistry of Ferro- and Ferriverdins. Iron Redox and Geometrical Stereodynamism

Partha Basu, Suranjan Bhanja Choudhury, Samudranil Pal, and Animesh Chakravorty*

Received November 28, 1988

Synthetic ferroverdins, $Fe(RQ)_3^-$ (**2**, R = Me, ^{t}Bu, Cl, Br), have been isolated as green sodium salts via iron(II)-promoted nitrosation of phenols. Bivalent ions (M^{2+}) displace Na^+ affording trinuclear $MFe_2(RQ)_6$, e.g., $MgFe_2(MeQ)_6$. The 1,2-quinone 2-oximato formulation (**2**) and *fac* geometry (**3a**) of $Fe(RQ)_3^-$ in $NaFe(RQ)_3$ are revealed by ^{1}H NMR spectra. Natural ferroverdin liberated by a species of *Streptomyces* differs from **2** only in the substituent R. Both Fe^{3+} and $Fe(bpy)_3^{3+}$ rapidly and quantitatively oxidize ferroverdin to ferriverdin, $Fe^{II}(RQ)_3^- \rightarrow Fe^{III}(RQ)_3$, with retention of *fac* geometry. The *fac*-$Fe(RQ)_3$ isomer (**4a**) so formed is however labile and spontaneously isomerizes to *mer*-$Fe(RQ)_3$ (**4b**; equilibrium population >85%). In contrast, the equilibrium concentration of *mer*-$Fe(RQ)_3^-$ (**3b**) in solutions of ferroverdin is estimated to be <0.5%. Both ferro- and ferriverdin are low spin: $S = 0$ and $^1/_2$, respectively. The EPR spectra of the latter in frozen-acetonitrile–toluene glass (77 K) are diagnostic of geometry: axial for *fac* (**4a**) and rhombic for *mer* (**4b**). The average axial and rhombic distortion parameters are 3800 and 0 cm^{-1}, respectively, for **4a** and 4900 and 2800 cm^{-1} for **4b**. The ground-state electronic configuration is e^4a^1 corresponding to $g_x, g_y < g_z$. In **4b**, an optical transition between two Kramers doublets is experimentally observable near 5600 cm^{-1}. The cycle of redox and isomerization equilibria

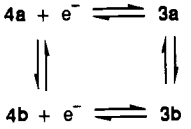

has been electrochemically mapped. It is possible to electrogenerate the $Fe(RQ)_3^z$ ($z = -1, 0$) species in a predetermined isomeric configuration at low temperature. The equilibrium constants [**3a**]/[**3b**] and [**4b**]/[**4a**] lie in the ranges 200–300 and 6–8, respectively, at 298 K. The formal potential (0.46–0.75 V vs SCE) of the *fac* couple, **4a**–**3a**, is more positive than that (0.27–0.55 V) of the *mer* couple, **4b**–**3b**. This correlates with the larger axial distortion of **4b** compared to **4a**. The rates of the isomerization reactions **3b** → **3a** and **4a** → **4b** have been followed spectrophotometrically for R = Me. Both processes are intramolecular and obey the first-order rate law. Their activation parameters (ΔH^*, kcal mol^{-1}; ΔS^*, eu) are 26.3 and 11.3 and 23.2 and 5.5, respectively. Mechanisms are unclear, but a twist pathway is chemically reasonable.

Introduction

Many microorganisms produce low molecular weight iron-specific chelating agents—usually polydentate hydroxamic acids or catechols—which strongly sequester the high-spin trivalent state of the metal, forming brown pseudooctahedal complexes having the FeO_6 coordination sphere.[1] A species of *Streptomyces*, however, generates a green pigment called ferroverdin in submerged cultures containing iron salts.[2] Here the chromophore is low-spin[2b] iron(II) tris chelated in N_3O_3 coordination by a "nitrosophenol" ligand as in **1**.[2d,3] In a single-crystal X-ray

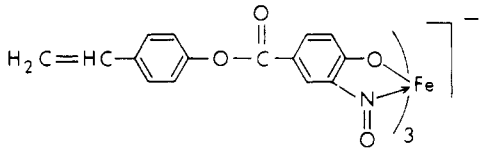

1

crystallographic study the countercation to **1** was found to be Na^+. The exact chemical composition of ferroverdin, however, varied in different preparations, and it was conjectured that countercation variation may be the reason.[3]

Work on ferroverdin chemistry was originally initiated by us with the objective of defining the nature and extent of the above-mentioned variation. Bivalent metal ions indeed replaced Na^+ in synthetic ferroverdins affording trinuclear $M^{II}Fe_2N_6O_6$ complexes. The focus of our attention however shifted when attempted trinucleation with Fe^{3+} failed to furnish the targeted mixed-valence $Fe^{III}Fe_2^{II}N_6O_6$ system and instead led to rapid oxidation of ferroverdin: $Fe^{II}N_3O_3 \rightarrow Fe^{III}N_3O_3$. Further scrutiny unfolded a dynamic relationship between metal oxidation state and tris chelate geometry. This constitutes the primary theme of the present paper.

Results and Discussions

A. Synthetic Ferroverdins: $NaFe(RQ)_3$. a. Synthesis and Characterization. The natural ferroverdin pigment was not available to us. Instead we have employed synthetic members (**2**) of the same chemical family—the ferroverdin family—differing

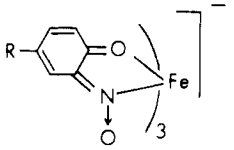

$Fe(RQ)_3^-$

R = Me, ^{t}Bu, Cl, Br

2

only in the substituent at 4-C. Green diamagnetic $NaFe(RQ)_3$ was prepared by the Baudisch–Cronheim reaction,[4-6] i.e., in situ nitrosation of the corresponding phenols in the presence of metal salts—iron(II) sulfate in the present case. Selected characterization data for the synthetic ferroverdins are collected in Table I. The electronic spectra of natural ferroverdin[2d,e] and **2** are very

(1) (a) Neilands, J. B., Ed. *Microbial Iron Metabolism*; Academic Press: New York, 1974. (b) Neilands, J. B. *Adv. Inorg. Biochem.* **1983**, *5*, 137. (c) Raymond, K. N.; Muller, G.; Matzanke, B. F. *Top. Curr. Chem.* **1984**, *123*, 49. (d) Hider, R. C. *Struct. Bonding* **1984**, *58*, 25. (e) Hossain, M. B.; Jalal, M. A. F.; Benson, B. A.; Barnes, C. L.; vander Helm, D. *J. Am. Chem. Soc.* **1987**, *109*, 4948–4954 and references therein.

(2) (a) Chain, E. B.; Tonolo, A.; Carilli, A. *Nature* **1955**, *176*, 645. (b) Ehrenberg, A. *Nature* **1956**, *178*, 379–380. (c) Ballio, A.; Bertholdt, H.; Chain, E. B.; Vittorio, V. D. *Nature* **1962**, *194*, 769–770. (d) Ballio, A.; Bertholdt, H.; Carilli, A.; Chain, E. B.; Vittorio, V. D.; Tonolo, A.; Vero-Bercellona, L. *Proc. R. Soc. London, B* **1963**, *158*, 43–70. (e) Neilands, J. B. *Struct. Bonding* **1966**, *1*, 59–108. (f) Ballio, A.; Barcellona, S.; Chain, E. B.; Tonolo, A.; Vero-Bercellona, L. *Proc. R. Soc. London, B* **1964**, *161*, 384–391.

(3) Candeloro, S.; Grdenič, D.; Taylor, N.; Thompson, B.; Viswamitra, M.; Hodgkin, D. C. *Nature* **1969**, *224*, 589–591.

(4) (a) Baudisch, O. *Science* **1940**, *92*, 336–337. (b) Cronheim, G. *J. Org. Chem.* **1947**, *12*, 1–29. (c) Sone, K. *Bull. Chem. Soc. Jpn.* **1952**, *25*, 1–7.

(5) (a) Carreck, P. W.; Charalambous, J.; Kensett, M. J.; McPartlin, M.; Sims, R. *Inorg. Nucl. Chem. Lett.* **1974**, *10*, 749–751. (b) Charalambous, J.; Frazer, M. J.; Sims, R. *Inorg. Chim. Acta* **1976**, *18*, 247–251. (c) Charalambous, J.; Haines, L. I. B.; Morgan, J. S.; Peat, D. S.; Campbell, M. J. M.; Baily, J. *Polyhedron* **1987**, *6*, 1027–1032.

(6) Chakravorty, A. *Coord. Chem. Rev.* **1974**, *13*, 1–46.

0020-1669/89/1328-2680$01.50/0

Table I. Characterization Data for $NaFe(RQ)_3$

compd	anal.,[a] % Fe	C	H	N	UV–vis data:[b] λ_{max}, nm (ϵ, M^{-1} cm^{-1})	^1H NMR spectral data:[c] δ (J, Hz) 3-H	5-H	6-H	4-R
$NaFe(MeQ)_3$	11.35 (11.47)	51.80 (51.76)	3.92 (3.96)	8.54 (8.63)	700 (6650), 445 (6700), 320[d] (11 950)	6.71[e] (2.2[f])	7.25 (2.3,[g] 9.1[h])	6.82 (9.1[i])	2.14
$NaFe(^tBuQ)_3$	9.01 (9.11)	58.70 (58.74)	5.81 (5.87)	6.69 (6.85)	700 (7900), 445 (7300), 330[d] (13 750)	6.81 (2.6[i])	7.52 (2.4,[g] 9.1[h])	6.84 (9.1[i])	1.12
$NaFe(ClQ)_3$	10.06 (10.19)	39.28 (39.39)	1.69 (1.60)	7.70 (7.90)	700 (7100), 450 (6950), 330[d] (11 950)	6.97 (2.2[i])	7.46 (2.5,[g] 9.2[h])	7.01 (9.1[i])	
$NaFe(BrQ)_3$	8.25 (8.20)	31.56 (31.69)	1.28 (1.32)	6.00 (6.16)	700 (8400), 450 (8400), 300[d] (14 800)	7.1 (1.8[i])	7.54[j] (9.0[h])	6.97 (9.1[i])	

[a] Calculated values are in parentheses. [b] Solvent is acetonitrile. [c] In $(CD_3)_2SO$. [d] Shoulder. [e] Center of a broad signal. [f] Coupling to 5-H resolved under double-resonance conditions (see text). [g] Coupling to 3-H. [h] Coupling to 6-H. [i] Coupling to 5-H. [j] Broad doublet with unresolved coupling to 3-H.

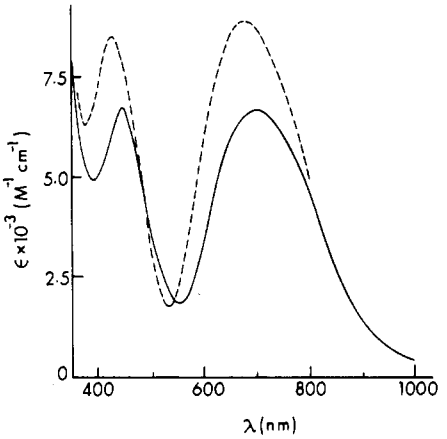

Figure 1. Electronic spectrum of $NaFe(MeQ)_3$ in acetonitrile (—). The spectrum of natural ferroverdin in methanol[2d,e] is superimposed for comparison (- - -).

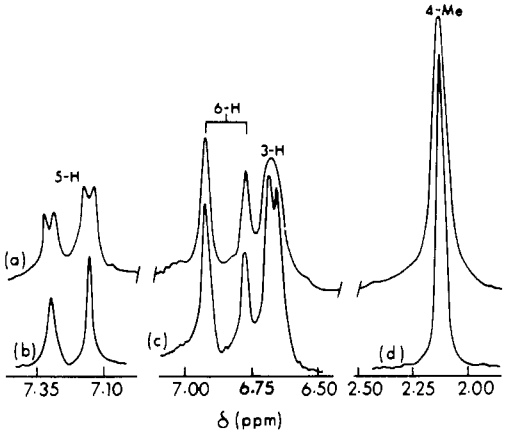

Figure 2. ^1H NMR spectra of $NaFe(MeQ)_3$ in $(CD_3)_2SO$ at 100 MHz: (a) normal spectrum; (b) 5-H signal after irradiation at δ 6.71 (3-H); (c) 6-H and 3-H signals after irradiation at δ 2.14 (4-Me); (d) 4-Me signal after irradiation at δ 6.71 (3-H).

similar and have characteristic bands near 450 and 700 nm (Figure 1).

b. Facial Geometry and Quinonoid Structure. The geometry of $Fe(RQ)_3^-$ and the 1,2-quinone 2-oximato formulation (**2**) are revealed by ^1H NMR spectra taken in dimethyl-d_6 sulfoxide. Measurements were carried out at both 100 and 270 MHz to distinguish between chemical shifts and spin–spin splittings. In natural ferroverdin the FeN_3O_3 coordination sphere is known[3] to be exclusiveiy *fac* (**3a**). In solutions of $NaFe(RQ)_3$, each kind

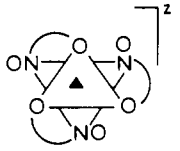

3a, $z = -1$
4a, $z = 0$

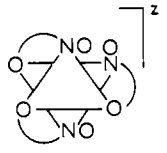

3b, $z = -1$
4b, $z = 0$

of proton has the same chemical shift for all three rings (Table I). Hence, the geometry of $Fe(RQ)_3^-$ is *fac* (**3a**), which, unlike the *mer* form (**3b**), has a C_3 axis.

The ^1H NMR spectrum of the R = Me complex is in Figure 2. The 3-H (δ 6.71) and the 4-Me signal (δ 2.14) are quite broad. Upon irradiation at δ 2.14, the 3-H signal sharpens and a small doublet splitting with $J \sim 2$ Hz becomes observable. When the 3-H signal is irradiated, the methyl resonance sharpens and the 5-H signal (δ 7.25) simplifies to a doublet (J = 9.1 Hz). The 6-H (δ 6.82) resonance remains a doublet (J = 9.1 Hz) throughout. Thus, 3-H is coupled to 4-Me and 5-H, and the latter is also coupled to 6-H. The observed allylic coupling between 3-H and 4-Me can arise only in the quinonoid structure **2**[7] but not in the aromatic nitrosophenolato structure (as in **1**).

Natural ferroverdin should also be formulated as a quinone oximate rather than as **1**. The reported bond distance data[3] are not in disagreement[6] with this proposal. The very close similarity between the visible spectra of natural and synthetic ferroverdins (Figure 1) further supports this. Crystallographic results on complexes of RQ^- with other metal ions have also shown the importance of the quinone oximato structure.[8]

c. Reaction with M^{2+}: Trinuclear Complexes. Upon reaction of $NaFe(RQ)_3$ with salts of bivalent metals in methanolic solution, sparingly soluble trinuclear $MFe_2(RQ)_6$ precipitates as a dark solid (M = Mg, Ca, Fe, Ni, Zn, Cd, etc). This strongly supports the contention that countercation variation is responsible for the compositional anomalies of natural ferroverdin preparations.[3] Trinuclearity is revealed by osmometric molecular weights in chloroform solution (e.g., for $MgFe_2(MeQ)_6$, calcd, 952.02; found, 917). Further details will be published elsewhere.[9-11]

B. Oxidation of Ferroverdin to Ferriverdin. Unlike Fe^{2+}, which leads to trinucleation, Fe^{3+} quantitatively oxidizes *fac*-$Fe(RQ)_3^-$ to $Fe(RQ)_3$.[12] The latter will be called ferriverdin. Exactly 1

(7) (a) Shoolery, J. N. *Varian Associates Tech. Bull.* **1957**, *2*, 18. (b) Roberts, J. D. *Nuclear Magnetic Resonance: Application to Organic Chemistry*; McGraw-Hill: New York, 1959; p 54.

(8) (a) McPartlin, M. *Inorg. Nucl. Chem. Lett.* **1973**, *9*, 1207–1210. (b) Korvenanta, J.; Saarinen, H. *Acta Chem. Scand., Ser. A* **1975**, *A29*, 861–865. (c) *Acta Chem. Scand., Ser. A* **1975**, *A29*, 409–413. (d) Bisi Castellani, C.; Gatti, G.; Millini, R. *Inorg. Chem.* **1984**, *23*, 4004–4008. (e) Bisi Castellani, C.; Carugo, O.; Coda, A. *Inorg. Chem.* **1987**, *26*, 671–675. (f) Bisi Castellani, C.; Carugo, O.; Coda, A. *Acta Crystallogr., Sect. C* **1988**, *C44*, 265–267. (g) Bisi Castellani, C.; Carugo, O.; Coda, A. *Acta Crystallogr., Sect. C* **1988**, *C44*, 267–270.

(9) We have not succeeded so far in growing single crystal of $MFe_2(MeQ)_6$ complexes. By analogy with trinuclear arylazooximates,[10,11] we propose that each *fac*-$Fe(RQ)_3^-$ moiety acts as a tridentate O_3 (oximato oxygen atoms) ligand and the M^{2+} ion is held in the grossly octahedral O_6 environment created by two such ligands.

(10) (a) Raghavendra, B. S. R.; Gupta, S.; Chakravorty, A. *Transition Met. Chem. (Weinheim, Ger.)* **1979**, *4*, 42–45. (b) Pal, S.; Chakravorty, A. *Inorg. Chem.* **1987**, *26*, 4331–4335.

(11) (a) Pal, S.; Melton, T.; Mukherjee, R. N.; Chakravarty, A. R.; Tomas, M.; Falvello, L. R.; Chakravorty, A. *Inorg. Chem.* **1985**, *24*, 1250–1257. (b) Pal, S.; Mukherjee, R. N.; Tomas, M.; Falvello, L. R.; Chakravorty, A. *Inorg. Chem.* **1986**, *25*, 200–207.

(12) It is conceivable that trinuclear species are formed transiently and provide a pathway for the very facile electron transfer. But we do not have any concrete evidence for this.

Table II. Characterization Data for $Fe(RQ)_3$

compd	anal.,[a] % Fe	C	H	N	μ_{eff},[b] μ_B	EPR g values[c] g_1	g_2	g_3	UV-vis data:[d] λ_{max}, nm (ϵ, M^{-1} cm^{-1})
$Fe(MeQ)_3$	12.00 (12.04)	58.71 (59.02)	4.14 (4.20)	8.89 (9.05)	1.80	2.307	2.160	1.971	970 (950), 570 (6700), 460 (9400), 350 (27 100)
$Fe(^tBuQ)_3$	9.52 (9.62)	61.80 (61.98)	4.55 (4.65)	7.18 (7.23)	1.79	2.307	2.159	1.971	970 (950), 580 (6300), 470 (7700), 340 (28 700)
$Fe(ClQ)_3$	10.51 (10.63)	41.10 (41.29)	1.71 (1.91)	7.99 (7.94)	1.86	2.306	2.155	1.967	980 (1050), 590 (6750), 470 (8900), 340 (28 500)
$Fe(BrQ)_3$	8.39 (8.48)	32.58 (32.78)	1.20 (1.37)	6.30 (6.37)	1.82	2.304	2.153	1.972	980 (950), 590 (6000), 460 (8300), 340 (28 000)

[a] Calculated values are in parentheses. [b] In the solid state at 298 K. [c] In dichloromethane–toluene (1:1) glass (77 K). [d] In dichloromethane.

Table III. EPR g Values,[a,b] Distortion Parameters, and Near-IR Transitions

compd	isomer	g_x	g_y	g_z	k	Δ/λ	V/λ	$\Delta E_1/\lambda$	$\Delta E_2/\lambda$ calcd	$\Delta E_2/\lambda$ obsd[c]
$Fe^{III}(MeQ)_3$	*fac*	−2.263	−2.263	1.959	1.23	9.287	0.000	8.900	9.840	
	mer	−2.294	−2.159	1.971	1.26	12.013	−6.693	8.710	15.458	13.50
$Fe^{III}(^tBuQ)_3$	*fac*	−2.267	−2.267	1.960	1.27	9.452	0.000	9.063	10.008	
	mer	−2.283	−2.159	1.971	1.23	11.828	−6.185	8.776	15.022	13.50
$Fe^{III}(ClQ)_3$	*fac*	−2.259	−2.259	1.960	1.22	9.391	0.000	9.003	9.947	
	mer	−2.296	−2.150	1.970	1.22	11.951	−7.266	8.366	15.680	13.75
$Fe^{III}(BrQ)_3$	*fac*	−2.263	−2.263	1.965	1.34	10.190	0.000	9.793	10.742	
	mer	−2.291	−2.155	1.975	1.35	13.143	−7.578	9.394	17.020	14.00

[a] Symbols have the same meanings as in the text. [b] In acetonitrile–toluene (1:1) glass (77 K). [c] Observed frequency (see text) converted to $\Delta E_2/\lambda$ by setting λ = 400 cm^{-1}.

mol of Fe^{3+} is required for complete oxidation of each mole of *fac*-$Fe(RQ)_3^-$. Evidences presented in later sections reveal that the oxidation step is fast and stereoretentive (eq 1). This is

$$fac\text{-}Fe(RQ)_3^- + Fe^{3+} \xrightarrow{fast} fac\text{-}Fe(RQ)_3 + Fe^{2+} \quad (1)$$

$$fac\text{-}Fe(RQ)_3 \rightleftharpoons mer\text{-}Fe(RQ)_3 \quad (2)$$

followed by a relatively slow *fac* → *mer* isomerization of ferriverdin (eq 2). At equilibrium, the *mer* isomer is present in large excess (>85%). The oxidation of ferroverdin to ferriverdin can also be achieved by $Fe(bpy)_3^{3+}$ (bpy = 2,2′-bipyridine) (eq 3) as well as electrochemically (vide infra).

$$fac\text{-}Fe(RQ)_3^- + Fe(bpy)_3^{3+} \xrightarrow{fast} fac\text{-}Fe(RQ)_3 + Fe(bpy)_3^{2+} \quad (3)$$

Ferriverdin has been isolated in high yields as dark brown solids[13] by oxidizing $NaFe(RQ)_3$ by ferric perchlorate in acetone or acetonitrile solutions. Single crystals of the complexes have eluded us. Their solution behavior is the same as that of the oxidized solutions (after equilibriation) considered above. Characterization data for the isolated complexes are collected in Table II. The complexes are low spin (t_2^5, $S = {}^1/_2$), which is unusual for N_3O_3-coordinated iron(III).[14] Because of this fortunate situation it has been possible to utilize X-band EPR spectra for unequivocal characterization of isomer geometry and electronic structure in a straightforward manner.[11,15,16]

C. EPR Spectra of Ferriverdin. a. Isomer Characterization. Solutions of $NaFe(RQ)_3$ in acetonitrile were oxidized chemically (Fe^{3+},[17] $Fe(bpy)_3^{3+}$) or electrochemically, and the EPR spectra of the solutions were recorded as a function of time after freezing aliquots to glass[18] at 77 K. Three stages of time evolution of spectra are displayed in Figure 3 for the R = Me complex. The initial spectrum is axial, corresponding to *fac*-$Fe(MeQ)_3$, which has a C_3 axis (**4a**). Thus the primary oxidation step is stereoretentive. With time, the $g_\perp$ intensity of *fac*-$Fe(MeQ)_3$ decreases and two new resonances, viz., g_2 (between $g_\parallel$ and $g_\perp$) and g_3 (near $g_\parallel$), appear due to the formation of the unsymmetrical *mer* form by spontaneous isomerization. The *mer* g_1 signal lies close to $g_\perp$. At equilibrium only 10–15% of the *fac* isomer is present (see below), and the rhombic features of the *mer* isomer dominate the spectrum. The EPR spectra (77 K) of solutions prepared by dissolving solid $Fe(RQ)_3$ in dichloromethane (Table II) are very closely similar to the above equilibrium spectrum.

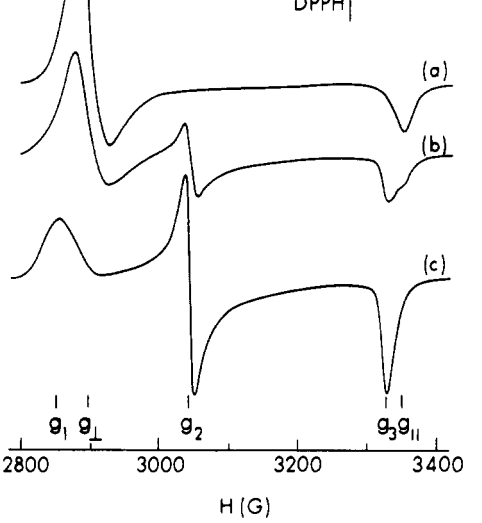

Figure 3. Time evolution of the EPR spectrum of $Fe(MeQ)_3$ showing the *fac* to *mer* convertion. The complex was produced in acetonitrile solution by oxidizing $NaFe(MeQ)_3$ with ferric perchlorate; aliquots were mixed with toluene (see text) and then frozen to 77 K. The approximate time intervals between oxidation and freezing are (a) 10 s, (b) 10 min, and (c) 2 h (equilibrium condition).

The g values of the geometrical isomers for the four ferriverdins generated by in situ oxidation of ferroverdins are listed in Table III. For the *fac* isomer $g_x = g_y = g_\perp$ and $g_z = g_\parallel$. From the nature of the spectra (Figure 3), it is clear that for the *mer* isomer the

(13) The synthesis (by a different route), magnetic susceptibility and Mössbauer spectra of a few tris(quinone oximato) iron(III) complexes have been reported.[5b] Their geometric configurations have not been defined.

(14) Gouzerh, P.; Jeannin, Y.; Rocchiccioli-Deltcheff, C.; Valentini, F. *J. Coord. Chem.* **1979**, *6*, 221–223.

(15) The EPR spectra of high-spin iron(III) complexes are complicated by zero-field splitting and associated phenomena.[16]

(16) (a) Blumberg, W. E. In *Magnetic Resonance in Biological Systems*; Ehrenberg, A., Vanngard, T., Eds.; Pergamon Press: New York, 1967; pp 119–133. (b) Peisach, J.; Blumberg, W. E.; Lode, E. T.; Coon, M. J. *J. Biol. Chem.* **1971**, *246*, 5877–5881. (c) Aasa, R. *J. Chem. Phys.* **1970**, *52*, 3919–3930. (d) Dowsing, R. D.; Gibson, J. F. *J. Chem. Phys.* **1969**, *50*, 294–303.

(17) By the use of a ferrous perchlorate solution as control, it was demonstrated that the Fe^{2+} ion produced by reduction of Fe^{3+} is EPR-silent under the experimental conditions. A 10-fold excess of ferric perchlorate did not affect the nature or intensity of EPR responses in any way showing that the entire *fac*-$Fe(MeQ)_3$ complex is formed within the time of mixing.

(18) To facilitate glass formation, an equal volume of toluene was added just before freezing.

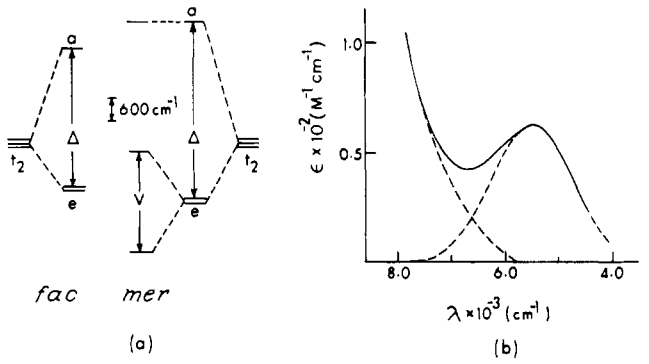

Figure 4. (a) Average axial (Δ) and rhombic (V) splittings of the t_2 level for the isomers of $Fe(RQ)_3$. (b) Near-IR spectrum (—) of $Fe(ClQ)_3$ in dichloromethane solution and Gaussian resolution (- - -).

g_3 resonance can be identified with g_z. We have also set $g_x = g_1$ and $g_y = g_2$.[19]

b. Electronic Structure of Isomers. The EPR g values can be used to probe the electronic ground state and distortion parameters of the $Fe(RQ)_3$ isomers. Distortions from O_h symmetry are measured in terms of axial (Δ) and rhombic (V) components. In the *fac* isomer $V = 0$ and Δ splits the octahedral t_2 state into a and e components. The *mer* isomer has only C_1 symmetry and both Δ and V are nonzero; here, V splits e into nondegenerate components, and the perpendicular resonance is correspondingly split into distinct g_x and g_y components. The distortion parameters can be quantitated using the **g** tensor theory of low-spin d^5 complexes.[20,21]

Selected results are collected in Table III and additional information is deposited in supplementary Table VII. Here k is the orbital reduction factor,[22-24] λ is the spin–orbit coupling constant and ΔE_1 and ΔE_2 are the ligand field transition energies from the EPR-active ground Kramers doublet to the upper two. The three doublets originate from the t_2 shell under the influence of Δ, V, and λ.[20,21] The positive sign of Δ corresponds to the case $g_x, g_y > g_z$. The a orbital lies above the e orbital, and the ground state is e^4a^1. The *mer* isomer is electronically more distorted than the *fac* isomer in both axial and rhombic senses. The orbital splitting of t_2 due to Δ and V and the average magnitudes of the latter are displayed in Figure 4a. The value of λ is taken as 400 cm^{-1}.[25] The average values of ΔE_1 and ΔE_2 (Table III) are respectively 3800 and 4100 cm^{-1} for the *fac* isomer and 3500 and 6300 cm^{-1} for the *mer* isomer.

Equilibriated solutions (>85% *mer*) of $Fe(RQ)_3$ produced by oxidation of *fac*-$Fe(RQ)_3^-$ or prepared by dissolving solid $Fe(RQ)_3$ display a relatively weak band in the near-IR region (Figure 4b). This is assigned to the ΔE_2 transition of the *mer* isomer. The agreement between the experimental and calculated ΔE_2 values (Table III) is quite satisfactory.[26] The ΔE_1 transition of the *mer* isomer and both the transitions of the *fac* isomer lie outside the range of our measuring instrument. The trend in the transition energies of the two isomers is revealed by Figure 4a. The ΔE_2 transition involving the lowest and the highest levels is augmented in energy in the *mer* form due to the contribution from the V parameter.

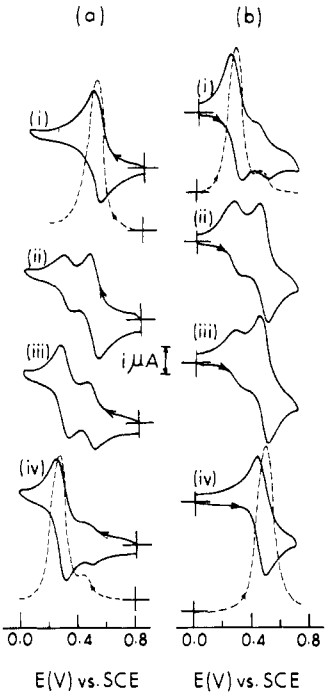

Figure 5. Time evolution (top to bottom) of cyclic and differential pulse voltammograms of isomerizing solutions ($\sim 10^{-3}$ M) at 298 K in acetonitrile (0.1 M TEAP) at a platinum working electrode. (a) $Fe(MeQ)_3$: (i) virtually pure *fac* isomer; (ii) and (iii) intermediate situations; (iv) equilibrium mixture of isomers (87% *mer*). (b) $Fe(MeQ)_3^-$: (i) a mixture of 87% *mer* and 13% *fac*; (ii) and (iii) intermediate situations; (iv) equilibrium mixture of isomers (>99.5% *fac*). Cyclic voltammetric scan rate is 50 mV s^{-1}; differential-pulse voltammograms have scan rate of 10 mV s^{-1} and modulation amplitude of 25 mV. The marked current range is 20 μA for cyclic voltammetry and 5 μA for differential-pulse voltammetry.

D. Redox and Isomerization Equilibria. a. The Cycle: Electrochemical Mapping. The oxidation of *fac*-ferroverdin to *fac*-ferriverdin and the subsequent isomerization of the latter can be visualized as segments of the thermodynamic redox-isomerization cycle covered by eq 4 and 5. Here $E°(fac)$ and $E°(mer)$

$$\begin{array}{ccc} fac\text{-}Fe(RQ)_3 + e^- & \overset{E°(fac)}{\rightleftharpoons} & fac\text{-}Fe(RQ)_3^- \\ k^{III}_b \Big\downarrow\Big\uparrow k^{III}_f & & k^{II}_f \Big\downarrow\Big\uparrow k^{II}_b \\ mer\text{-}Fe(RQ)_3 + e^- & \overset{E°(mer)}{\rightleftharpoons} & mer\text{-}Fe(RQ)_3^- \end{array} \quad (4)\ (5)$$

are the formal potentials of the couples of eq 4 and 5, respectively. The forward (f) as opposed to the backward (b) direction of each isomerization equilibrium is taken as the direction in which the reaction is favorable. This happens to be *fac* → *mer* in the case of $Fe(RQ)_3$ (eq 2) and *mer* → *fac* (see below) in the case of $Fe(RQ)_3^-$. The isomerization rate constants k^{III}(ferriverdin) and k^{II}(ferroverdin) are given the subscripts f and b accordingly. The constants of the isomerization equilibria defined in the above manner are given by eq 6 and 7.

$$K^{III} = k^{III}_f/k^{III}_b = [mer\text{-}Fe(RQ)_3]/[fac\text{-}Fe(RQ)_3] \quad (6)$$

$$K^{II} = k^{II}_f/k^{II}_b = [fac\text{-}Fe(RQ)_3^-]/[mer\text{-}Fe(RQ)_3^-] \quad (7)$$

The $E°$'s and K's of the above cycle have been determined electrochemically (platinum electrode) in acetonitrile solution. The cyclic voltammogram (couple of eq 4) of $NaFe(RQ)_3$ consists of a reversible one-electron response with peak-to-peak separation of 60 mV (263–308 K). The geometric structure of the complex

(19) Interchange of g_x and g_y merely changes the sign of the rhombic distortion parameter (V, see text) and does not affect anything else.

(20) (a) Bleaney, B.; O'Brien, M. C. M. *Proc. Phys. Soc. London, Sect. B* **1956**, *69*, 1216–1230. (b) Griffith, J. S. *The Theory of Transition Metal Ions*; Cambridge University Press: London, 1961; p 364.

(21) (a) Bhattacharya, S.; Chakravorty, A. *Proc. Indian Acad. Sci., Chem. Sci.* **1985**, *95*, 159–167. (b) Bhattacharya, S.; Ghosh, P.; Chakravorty, A. *Inorg. Chem.* **1985**, *24*, 3224–3230. (c) Lahiri, G. K.; Bhattacharya, S.; Ghosh, B. K.; Chakravorty, A. *Inorg. Chem.* **1987**, *26*, 4324–4331. (d) Lahiri, G. K.; Bhattacharya, S.; Mukherjee, M.; Mukherjee, A. K.; Chakravorty, A. *Inorg. Chem.* **1987**, *26*, 3359–3365.

(22) Normally k should be less than 1.0, but in an analysis of the present type, k acts as a sink for various unaccounted effects including mixing with excited states which can lead to $k > 1$.[23] This situation often arises when g_x lies close to 2.[24]

(23) (a) Hill, N. J. *J. Chem. Soc., Faraday Trans.* **1972**, *68*, 427–434. (b) Cotton, S. A. *Inorg. Nucl. Chem. Lett.* **1972**, *8*, 371–373. (c) DeSimone, R. E. *J. Am. Chem. Soc.* **1973**, *95*, 6238–6244.

(24) Chakravarty, A. R.; Chakravorty, A. *J. Chem. Soc., Dalton Trans.* **1982**, 615–622.

(25) Cotton, S. A.; Gibson, J. F. *J. Chem. Soc. A.* **1971**, 803–809.

(26) The calculations are based on $\lambda = 400$ cm^{-1}. If the value of λ is somewhat lower, the agreement improves considerably. The agreement becomes nearly perfect at $\lambda = 360$ cm^{-1}. But in approximations of the present kind perfect agreement is of no special significance.

Table IV. Cyclic Voltammetric Formal Potentials of Isomers in Acetonitrile (0.1 M TEAP) at a Platinum Electrode[a-c]

R	temp, K	$E°_{fac}$, V (ΔE_p, mV)	$E°_{mer}$, V (ΔE_p, mV)
Me	263	0.46 (60)	0.27 (80)
	281	0.46 (80)	0.27 (80)
	298	0.45 (60)	0.26 (80)
	308	0.46 (60)	0.27 (80)
^{t}Bu	263	0.48 (60)	0.29 (60)
	298	0.48 (60)	0.29 (60)
Cl	263	0.73 (60)	0.53 (70)
	298	0.72 (60)	0.53 (60)
Br	263	0.74 (60)	0.55 (70)
	298	0.75 (60)	0.55 (70)

[a] Scan rate 50 mV s^{-1}. [b] $E°$ is equal to the average of anodic (E_{pa}) and cathodic (E_{pc}) peak potentials. [c] $\Delta E_p = E_{pa} - E_{pc}$.

Table V. Equilibrium Constants in Acetonitrile Solution at 298 K

R	$10^{-3}K^{Cr}$ [a]	K^{III} [b]	$10^{-2}K^{II}$ [a]
Me	1.6	6.5	2.5
^{t}Bu	1.6	5.7	2.9
Cl	1.6	7.9	2.1
Br	2.4	8.0	3.0

[a] From eq 9. [b] From differential-pulse voltammetry.

is conserved on the cyclic voltammetric time scale. Coulometric oxidation takes a much longer time, and if performed at 298 K, the resultant solution shows (e.g., EPR evidence) the presence of substantial amounts of *mer*-$Fe(RQ)_3$ evidently formed by isomerization of the electrogenerated *fac* form. The isomerization process becomes very slow at 263 K, and cold solutions of virtually pure *fac*-$Fe(RQ)_3$ can be generated by doing coulometry at this temperature. If this solution is now quickly warmed to 298 K and left to isomerize, the cyclic and differential pulse voltammograms evolve with time as shown in Figure 5a (R = Me). The progressive replacement of the *fac* response (eq 4) by the *mer* response (eq 5) occurring at lower potential is clearly observable. At equilibrium the predominant isomer is *mer*-$Fe(RQ)_3$. The EPR spectrum (77 K) of this solution (R = Me) is the same as that shown in Figure 3c. The voltammogram of solution prepared by dissolving solid $Fe(MeQ)_3$ is the same as that of Figure 5a(iv).

When the above equilibriated solution of $Fe(RQ)_3$ is coulometrically reduced at 263 K, $Fe(RQ)_3^-$ is quantitatively regenerated. The isomer distribution is unaffected by reduction (very slow isomerization), and the cyclic voltammogram of the cold reduced solution (initial scan anodic) is the same as that of equilibriated $Fe(RQ)_3$ parent (initial scan cathodic, Figure 5a(iv)). Thus a solution containing metastable *mer*-$Fe(RQ)_3^-$ as the major constituent can be prepared at 263 K. When the solution is left to isomerize at 298 K, the concentration of the *fac* isomer increases progressively, and at equilibrium the *mer* response is unobservable (Figure 5b, R = Me). The final voltammogram (Figure 5b(iv)) is identical with that of the original starting material, i.e., $NaFe(RQ)_3$.

The formal potentials of the isomers are listed in Table IV. For a given complex, there is virtually no variation of the potentials in the temperature range 263–308 K. The potentials increase substantially in going from R = alkyl to R = halogen as expected. The reduction potentials of Fe^{3+} (in ferric perchlorate) and $Fe(bpy)_3^{3+}$ in acetonitrile are 0.7[27] and 1.06 V[28] respectively. These two reagents are therefore able to oxidize *fac*-$Fe(RQ)_3^-$ (eq 1 and 3).

b. Equilibrium Constants. The constant K^{III} was conveniently determined from differential-pulse voltammograms (Figure 5), and data are listed in Table V. The population of *mer*-$Fe(RQ)_3$ is >85% at equilibrium in acetonitrile solution (298 K).

Neither ^{1}H NMR spectra nor voltammograms revealed the presence of the *mer* isomer in solutions of $NaFe(RQ)_3$. The

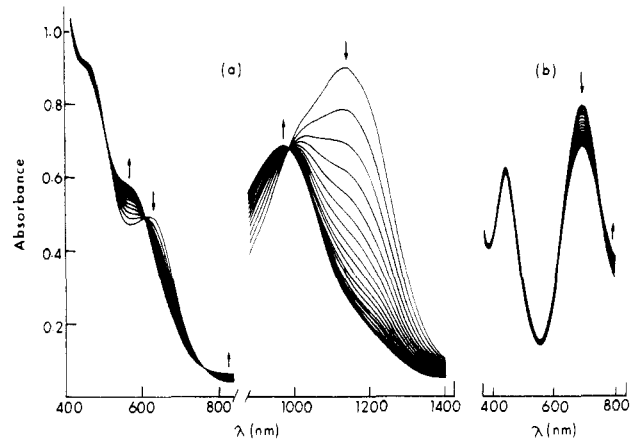

Figure 6. Electronic spectra of isomerizing solutions of (a) $Fe(MeQ)_3$ and (b) $Fe(MeQ)_3^-$ in acetonitrile at 298 K. The arrows indicate increase and decrease of band intensities as reaction proceeds.

equilibrium concentration of this isomer must therefore be small. The constant K^{II} can be estimated by considering the redox cross-reaction of eq 8 having the equilibrium constant K^{cr} (eq 9).

$$fac\text{-}Fe(RQ)_3 + mer\text{-}Fe(RQ)_3^- \rightleftharpoons fac\text{-}Fe(RQ)_3^- + mer\text{-}Fe(RQ)_3 \quad (8)$$

$$K^{cr} = K^{III}K^{II} = \exp\left[\frac{F}{RT}(E°_T(fac) - E°_T(mer))\right] \quad (9)$$

Since K^{III} and the two formal potentials are known, K^{II} can be computed. Results are shown in Table V. The concentration of *mer*-$Fe(RQ)_3^-$ at equilibrium is <0.5% in acetonitrile (298 K). The values of K^{cr} (Table V) reflect the superior thermodynamic stabilities of *mer*-$Fe(RQ)_3$ and *fac*-$Fe(RQ)_3^-$. It also reflects (eq 9) that *fac*-ferriverdin is a more potent oxidant than its *mer* congener.

A comment on the relative stabilities of the isomers is in order. In general the *mer* geometry should be sterically more favorable than the *fac* geometry since the pendant oximato oxygen atoms have greater separation in the former. If ligand distribution were statistical, we should have $K^{III} = 3$. Observed K^{III} values are substantially larger (Table V) and this could at least, in part, be due to the above-mentioned steric factor. However this factor cannot explain the large stability of *fac*-$Fe(RQ)_3^-$ (very small K^{II}). The origin of this is probably electronic and is under further scrutiny.[29,30]

c. Rates of Isomerization. In the cycle of eq 4 and 5 the only parameters remaining to be estimated are the isomerization rates. Since K^{III} and K^{II} are known, only two of the rate constants such as k^{III}_f and k^{II}_f are actually required to be determined. This has been achieved in the case of R = Me species.

To determine k^{III}_f, *fac*-$Fe(RQ)_3$ was generated chemically or coulometrically in acetonitrile solution. With time its moderately intense bands at 1140 and 640 nm are replaced by those of the *mer* isomer at 900 and 590 nm (see also Table II).[31] The time evolution of the spectrum is characterized by well-defined isosbestic points (Figure 6). The rate process is first order with respect to the complex and is independent of the concentration and nature of the oxidant as well as of added salt concentration (0.0 and 0.1 M TEAP were used).

To measure k^{II}_f, the isomerization of electrogenerated *mer*-$Fe(RQ)_3^-$ in acetonitrile was monitored (Figure 6). Both isomers have an allowed band at 690 nm, but the *fac* band is broader and

(27) Cathodic peak potential of ferric perchlorate in acetonitrile determined by cyclic voltammetry.
(28) Weiner, M. A.; Basu, A. *Inorg. Chem.* **1980**, *19*, 2797–2800.
(29) An extended Huckel molecular orbital study[30] on $Mo(CO)_3(PH_3)_3^z$ has revealed that the stable 18e ($z = 0$, t_2^6) and 17e ($z = 1$, t_2^5) geometries are respectively *fac* and *mer*. We note that $Fe(RQ)_3^z$ ($z = 0, -1$) also form a 18e–17e pair.
(30) Mingos, D. M. P. *J. Organomet. Chem.* **1979**, *179*, C29–C33.
(31) The EPR signals and voltammetric response of the *mer* isomer grow parallely. The spectrophotometric method affords the most convenient and accurate way to follow the rates quantitatively.

Table VI. Rate Constants and Activation Parameters in Acetonitrile

complex	temp, K	rate const, s^{-1}	$\Delta H^{\ddagger}$, kcal/mol	$\Delta S^{\ddagger}$, eu	E_a, kcal/mol	log A
$Fe(MeQ)_3^{-a}$	296	0.92×10^{-4}	26.29	11.27	26.90	15.69
(*mer* → *fac*)	301	1.58×10^{-4}				
	307	5.04×10^{-4}				
	314	11.17×10^{-4}				
$Fe(MeQ)_3^{b}$	287	0.32×10^{-3}	23.20	5.49	23.90	14.50
(*fac* → *mer*)	292	0.47×10^{-3}				
	299	1.37×10^{-3}				
	305	2.68×10^{-3}				
	292	0.49×10^{-3}				
	299	1.35×10^{-3}				
	305	2.77×10^{-3}				
	292	0.50×10^{-3}				
	296	0.93×10^{-3}				
	302	2.37×10^{-3}				
	308	5.14×10^{-3}				

[a] The *mer* isomer (87%) was produced coulometrically. [b] The *fac* isomer was variously produced: for the first four data points, oxidation by 1 equiv of Fe^{3+}; for the next three data points, oxidation by 2 equiv of Fe^{3+}; for the last four data points, oxidation by coulometry.

has a lower extinction coefficient. The rate is first order with respect to the complex.

Variable-temperature rate constants and derived activation parameters are collected in Table VI ($\Delta H^{\ddagger}$, enthalpy; $\Delta S^{\ddagger}$, entropy; E_a, energy; log A, frequency factor). The parameters show no dramatic dependence on oxidation state. The entropy factor favors k^{II}_f over k^{III}_f, but the enthalpy factor is controlling and it favors k^{III}_f more. In effect k^{II}_f is 1 order of magnitude smaller than k^{III}_f. The rate constants of the backward reactions calculated with the help of equilibrium constants are $k^{II}_b = 4.4 \times 10^{-7}$ s^{-1} and $k^{III}_b = 1.4 \times 10^{-4}$ s^{-1} (both at 298 K).

When mixtures (e.g., R = Me and Cl) are allowed to coisomerize, no mixed ligand complexes of the type $Fe(MeQ)_n(ClQ)_{3-n}^z$ (n = 1, 2; z = −1, 0) are formed. The electrochemical response of the solution corresponds throughout only to pure tris chelates (n = 0, 3). The isomerization process is thus *intramolecular* in nature. Such a process can proceed via bond-breaking and/or twist pathways. Unfortunately activation parameters are often not good discriminators of the possible alternatives.[32] The RQ^- ligand is rigid and planar and this may make the twist pathway favorable for $Fe(RQ)_3^z$.[33]

d. Formal Potential and Axial Distortion of Isomers. The formal potentials of the isomers (Table IV) follow eq 10 where α lies close to 190 mV. The relationship of eq 10 can be qualitatively rationalized in terms of axial distortion (Δ). In the reduction of $Fe(RQ)_3$ (t_2^5) to $Fe(RQ)_3^-$ (t_2^6), an electron is added to the a orbital that is half-filled (a^1) in $Fe(RQ)_3$ and is fully occupied (a^2) in $Fe(RQ)_3^-$. Since $\Delta(fac) < \Delta(mer)$, the a orbital is more stable in the *fac* isomer (Figure 4a), which is thus more easily reduced (more positive $E°_{298}$).

$$E°_{298}(fac) = E°_{298}(mer) + \alpha \qquad (10)$$

The energy of the a orbital is approximately equal to $2\Delta/3$.[20,21] The stabilization(s) of this orbital in the *fac* isomer with respect to that in the *mer* isomer is thus expressed by eq 11. From the data of Table IV, the value of β is estimated to be ~100 mV. Thus β can be a major constituent of α.

$$\beta = \frac{2}{3}(\Delta(mer) - \Delta(fac)) \qquad (11)$$

Low-spin d^5–d^6 redox couples of *fac* and *mer* isomers are documented among carbonyl complexes of type $M(CO)_3L_3^z$ (M = Cr, Mn; L = monodentate ligand, weaker π-acceptor than CO). The $E°(fac) > E°(mer)$ relation is valid in these cases also.[34] Better π-stabilization (π-back-bonding to CO) of the redox orbital in the reduced (d^6) *fac* isomer is believed to be a reason.[35]

E. Concluding Remarks. The family of synthetic ferro- and ferriverdins reported in this work has provided model examples of the dependence of tris chelates geometry on metal oxidation state. To the best of our knowledge no parallel example exists in iron chemistry. In ferroverdins—$Fe(RQ)_3^-$—the low-spin bivalent metal displays a high degree of thermodynamic specificity for the *fac* geometry. On the other hand in ferriverdin—$Fe(RQ)_3$–low-spin iron(III) shows a good degree of preference for the *mer* geometry. The isomers with mismatch between geometry and oxidation state—*mer*-$Fe(RQ)_3^-$ and *fac*-$Fe(RQ)_3$—can be generated via rapid electron transfer. These strained systems relax by spontaneous isomerization, albeit slowly. All equilibrium and rate parameters defining the redox and isomerization phenomena have been quantitated. The axial and rhombic distortion parameters of ferriverdins have been measured. The order of axial distortion (*mer* > *fac*) is compatible with the order of $Fe(RQ)_3$–$Fe(RQ)_3^-$ formal potential: *mer* < *fac*. Ferroverdins are quinone oximate chelates and can sequester metal ions. This has provided a rationale for the reported compositional variation of natural ferroverdin.

The quinone oximates potentially provide an unique opportunity for studying the pattern of z-geometry relationship in the entire group of 3d transition metal ion complexes of the type $M(RQ)_3^z$ (z = 0, −1). The results for M = Ni were reported recently.[36] Trivalent nickel strongly favors the *mer* geometry (98% at equilibrium), but the bivalent metal is lax in its specificity for the *fac* form (56% at equilibrium). This is an antithesis to the behavior of $Fe(RQ)_3^z$. We have indications that in $Co(RQ)_3$ the *fac* geometry is strongly favored and $Mn(RQ)_3^z$ is *mer*, independent of z. The basis of such variations remains to be understood. Little is known at present about the Ti, V, and Cr complexes. Further studies are in progress.

Experimental Section

Physical Measurements. Microanalytical data (C, H, N) were obtained with a Perkin-Elmer Model 240C elemental analyzer. Molecular weights were determined in chloroform solution by using a Knauer vapor pressure osmometer with benzil as calibrant. Electronic spectra were recorded with a Hitachi 330 spectrophotometer. ^1H NMR spectra were collected in $(CD_3)_2SO$ by using JEOL 100-MHz and Bruker 270-MHz spectrometers. Magnetic susceptibilities were measured on a PAR-155 vibrating-sample magnetometer fitted with a Walker Scientific magnet. EPR spectra were recorded in the X-band on a Varian E-109C spectrometer fitted with a quartz Dewar for measurements at 77 K (liquid nitrogen). The spectra were calibrated with respect to DPPH (g = 2.0037). Electrochemical measurements were done by using the PAR Model 370-4 electrochemistry system incorporating the following: Model 174A polarographic analyzer; Model 175 universal programmer; Model RE0074 XY recorder; Model 173 potentiostat; Model 179 digital coulometer; Model 377 cell system. A planner Beckman Model 39273 platinum-inlay working electrode, a platinum-wire auxiliary electrode, and an aqueous saturated calomel reference electrode (SCE) were used in three-electrode measurements. A platinum-wire-gauge working electrode was used in coulometric experiments. All experiments were performed under dinitrogen atmosphere, and reported potentials are uncorrected for junction contribution. Haake Model-F3K and Model-D8G digital cryostats and circulators connected to appropriate jacketed cells were used for low-temperature electrochemical and spectrophotometric measurements.

Materials. Hydrated perchlorates of iron(II), iron(III), and magnesium(II) were prepared by dissolving iron powder, iron(III) hydroxide, and magnesium(II) carbonate, respectively, in 70% aqueous perchloric acid and then crystallizing the salts. Tris(2,2′-bipyridine)iron(III) perchlorate was prepared by a reported method.[37] The purification of acetonitrile and dichloromethane and the preparation of tetraethylammonium perchlorate (TEAP) for electrochemical/spectroscopic work

(32) Serpone, N.; Bickley, D. G. *Prog. Inorg. Chem.* **1972**, *17*, 391–566 and references therein.
(33) Basolo, F.; Hayes, J. C.; Newmann, H. M. *J. Am. Chem. Soc.* **1953**, *75*, 5102–5106.
(34) (a) Bond, A. M.; Grabaric, B. S.; Grabaric, Z. *Inorg. Chem.* **1978**, *17*, 1013–1018. (b) Bond, A. M.; Carr, S. W.; Colton, R.; *Inorg. Chem.* **1984**, *23*, 2343–2350. (c) Bond, A. M.; Colton, R.; Kevekordes, J. E. *Inorg. Chem.* **1986**, *25*, 749–746.
(35) Bursten, B. E. *J. Am. Chem. Soc.* **1982**, *104*, 1299–1304.
(36) Ray, D.; Chakravorty, A. *Inorg. Chem.* **1988**, *27*, 3292–3297.
(37) Burstall, F. H.; Nyholm, R. S. *J. Chem. Soc.* **1952**, 3570–3579.

were done as before.[21c] All other chemicals and solvents were used as obtained.

Preparation of Complexes. Sodium Tris(4-R-1,2-benzoquinone 2-oximato)ferrate(II), Na[Fe(RQ)$_3$]. There have been several mentions of green complexes of iron(II) with RQ^- in the literature,[4,5] but preparative details do not appear to have been documented. We report below the procedure for synthesizing the R = Me complex. By use of appropriate phenols, the other complexes were similarly prepared in similar yields.

A solution of 5.4 g (0.05 mol) of *p*-cresol in 15 mL of glacial acetic acid was diluted with 25 mL of water, and sufficient CH_3COONa was added to adjust the pH to ~4.2. An aqueous solution (125 mL) of 7.0 g (0.03 mol) of $FeSO_4 \cdot 7H_2O$ was then added. This was followed by the addition of a solution of 8.65 g (0.12 mol) $NaNO_2$ in 125 mL of water with continuous stirring. The mixture gradually became dark brown. It was then set aside for 7 days. The dark precipitate formed was collected by filtration, washed thoroughly with water, dried in vacuum over P_4O_{10}; yield 6.48 g (80%). The complex was recrystallized from alkaline (NaOH) aqueous acetone.

It is soluble in polar organic solvents such as acetone, acetonitrile, methanol, dimethyl sulfoxide, and dimethyl formamide but is insoluble in dichloromethane, chloroform, and benzene.

Bis[tris(4-methyl-1,2-benzoquinone 2-oximato)ferrato(II)]magnesium(II), $MgFe_2(MeQ)_6$. To a solution of $NaFe(MeQ)_3$ (0.40 g, 0.82 mmol) in methanol (20 mL) was added 0.15 g (0.45 mmol) of $Mg(ClO_4)_2 \cdot 6H_2O$, and the mixture was stirred magnetically for 1 h. The color of the solution changed rapidly from green to bluish green and a dark solid precipitated. This was collected by filtration, washed thoroughly with methanol followed by water, and dried in vacuum over P_4O_{10}; yield 0.32 g (82%).

Tris(4-R-1,2-benzoquinone 2-oximato)iron(III). These complexes were synthesized by oxidizing $NaFe(RQ)_3$ with iron(III) perchlorate.

We first consider the case of R = Cl. To a solution of $NaFe(ClQ)_3$ (1.0 g, 1.82 mmol) in acetone (20 mL) was added 0.95 g (2.05 mmol) of solid $Fe(ClO_4)_3 \cdot 6H_2O$. The solution color immediately changed from green to brown. The mixture was then stirred for 0.5 h, and a dark precipitate of $Fe(ClQ)_3$ was formed. It was collected by filtration and was washed with water and dried in vacuum over P_4O_{10}; yield 0.77 g (80%). The R = Br complex was prepared similarly from $NaFe(BrQ)_3$ and $Fe(ClO_4)_3 \cdot 6H_2O$; yield 75%.

For the synthesis of the R = Me complex, a suspension of $NaFe(MeQ)_3$ (0.49 g, 1.00 mmol) in dichloromethane (30 mL) was shaken with 30 mL of aqueous ferric perchlorate (0.939 g, 2.01 mmol) solution. The brown organic layer was then separated, filtered (to remove off solid particles, if any), washed with water, and finally evaporated in vacuum to dryness, affording the complex; yield 0.40 g (85%). The R = ^{t}Bu complex was prepared analogously.

Electrosynthesis of *fac*-Fe(RQ)$_3$ and *mer*-Fe(RQ)$_3^-$ in Solution. The case of R = Me is cited here. A 20-mL acetonitrile solution containing 3.5 mg (0.71 mmol) of $NaFe(MeQ)_3$ and 0.46 g (2.00 mmol) of TEAP was cooled to 263 K in the thermostated coulometric cell. The potential of the platinum gauze working electrode was fixed at 0.70 V. The oxidation was completed at a count of 0.683 C (the calculated count for one-electron oxidation was 0.684 C). The solution contains nearly pure *fac*-$Fe(MeQ)_3$.

An equilibriated solution of $Fe(MeQ)_3$ (5.1 mg, 1.10 mmol) in 20 mL acetonitrile containing 0.46 g of TEAP was cooled to 263 K and subjected to constant-potential (0.00 V) coulometric reduction. The reduction was complete at a count of 1.010 C (the calculated coulomb count for one electron transfer is 1.061 C). The solution so produced contains ~87% *mer*-$Fe(MeQ)_3^-$ and ~13% *fac*-$Fe(MeQ)_3^-$.

Treatment of EPR and Related Data. All five t_2 electrons were explicitly considered. The octahedral $^2T_2$ (t_2^5) ground state is split by Δ and V into $^2A_2$, $^2E_+$ and $^2E_-$,[38] and when λ is considered, three Kramers doublets emerge of which the EPR-active ground doublet can be written as in eq 12, where the terms with the bar on top have β-spin. Values of

$$\psi_i = p|E_+\rangle + q|\bar{A}\rangle + r|E_-\rangle \quad (12a)$$

$$\psi_{ii} = p|\bar{E}_-\rangle + q|A\rangle + r|\bar{E}_+\rangle \quad (12b)$$

p, q, r, and k are extracted by fitting observed g values to eq 13–15 and

$$g_x/2 = -2pr - q^2 - 2^{1/2}kq(p + r) \quad (13)$$

$$g_y/2 = 2pr - q^2 - 2^{1/2}kq(p - r) \quad (14)$$

$$g_z/2 = -p^2 + q^2 - r^2 - k(p^2 - r^2) \quad (15)$$

using the normalization condition $p^2 + q^2 + r^2 = 1$. One then proceeds to compute Δ, V, ΔE_1, and ΔE_2. Further details have been elaborated elsewhere.[21]

The Gaussian analysis of the near-IR band (ΔE_2) was done by trial and error with the help of eq 16, where ϵ_ν and ϵ_0 are extinction coefficients at frequencies ν and ν_0 (band maxima), respectively, and δ is the full width at half-height.[39]

$$\epsilon_\nu = \epsilon_0 \exp[-5.545(\nu - \nu_0)^2/2\delta^2] \quad (16)$$

Kinetic Measurements. Solutions of the reactive isomers were produced chemically, or electrochemically isomerization was monitored spectrophotometrically in thermostated 1-cm cells. For the determination of k^{III}_f, the absorbance at 1140 nm was digitally recorded as a function of time (t). The relevant rate equation[40] is given by eq 17, where A_0, A_t

$$-\log (A_t - A_\infty) = \frac{K^{III}_f A_0 t}{2.303(A_0 - A_\infty)} - \log (A_0 - A_\infty) \quad (17)$$

and A_∞ are absorbances at $t = 0$, $t = t$ and $t = \infty$ (i.e., at equilibrium). The rate constant k^{III}_f was obtained from linear least-squares plots of $-\log (A_t - A_\infty)$ against t. A minimum of 30 $A_t - t$ data points were used in each calculation. The activation parameters $\Delta H^\ddagger$ and $\Delta S^\ddagger$ were obtained from the Eyring plot while E_a and log A were obtained from the Arrhenius plot.

Determination of k^{II}_f was achieved by following the absorption at 690 nm. The treatment of data is analogous to that used in the case of k^{III}_f.

Acknowledgment. Financial assistance received from the Council of Scientific and Industrial Research and Department of Science and Technology, New Delhi, India, is gratefully acknowledged. We are thankful to Professor R. P. Gandhi for some of the ^{1}H NMR spectra.

Supplementary Material Available: Complete results of EPR analysis of $Fe(RQ)_3$ complexes (Table VII) (2 pages). Ordering information is given on any current masthead page.

(38) Sugano, S.; Taube, Y.; Kamimura, H. *Multiplets of Transition Metal Ions in Crystals*; Academic Press: New York, 1970; p 131.
(39) Barker, B. E.; Fox, M. F. *Chem. Soc. Rev.* **1980**, *9*, 143–184.
(40) Wilkins, R. G. *The Study of Kinetics and Mechanism of Reactions of Transition Metal Complexes*; Allyn and Bacon, Inc.: Boston, 1974; pp 16–18.